

Alternate computational method for induction disk motor based on 2D FEM model of cylindrical motor

TOMASZ WOLNIK 

*Lukasiewicz Research Network, Institute of Electrical Drives and Machines KOMEL
Al. Roździeńskiego 188, 40-203 Katowice, Poland
e-mail: t.wolnik@komel.com.pl*

(Received: 27.08.2019, revised: 19.11.2019)

Abstract: Disk motors are characterized by the axial direction of main magnetic flux and the variable length of the magnetic flux path along varying stator/rotor radii. This is why it is generally accepted that reliable electromagnetic calculations for such machines should be carried out using the FEM for 3D models. The 3D approach makes it possible to take into account an entire spectrum of different effects. Such computational analysis is very time-consuming, this is in particular true for machines with one magnetic axis only. An alternate computational method based on a 2D FEM model of a cylindrical motor is proposed in the paper. The obtained calculation results have been verified by means of lab test results for a physical model. The proposed method leads to a significant decrease of computational time, i.e. the decrease of iterative search for the most advantageous design.

Key words: computational methods, disk motors, induction motors

1. Introduction

Nowadays the global market of electrical machines is dominated by machines with the cylindrical design of an electromagnetic circuit. The design and manufacturing process of such machines have been thoroughly documented by researchers and constructors in the last decades [1, 2]. Still, there are some applications where the use of standard cylindrical machines is difficult or not very effective from economic or technical point of view. An interesting alternative emerges in the form of disk motors which may provide a better solution to a given problem in selected cases just on account of the specific shape of an electromagnetic circuit [3–6].

In disk induction motors, the analysis of an electromagnetic circuit is more complex than in standard cylindrical machines. The length of the magnetic path of the main magnetic flux varies at the diameters of stator and rotor disks [7–10]. For the inner diameter the length of the magnetic path is the shortest, while for the outer diameter it is the longest. Moreover, some constructional



elements of electromagnetic circuits (e.g. stator and rotor teeth) have different cross-sections and dimensions along the variable diameter. Hence, it is assumed that calculations of electromagnetic circuits of disk induction motors should be carried out with methods taking into account all issues listed above. The 3D FEM is one such method. However, this method requires appropriate computing power and it is very time-consuming in particular when calculations of a complete motor model are necessary. Any optimization procedures are possible only when there is no enforced time limit. This is a significant problem for designers of such machines.

An alternative computational method for an induction disk motor with a single stator and single rotor (AFIM-11) is presented in this paper. It is established based on the analysis of an electromagnetic circuit by the 2D finite element method. Since the principle of the operation as well as the equivalent scheme (Fig. 1) of a disk induction motor are the same as those of a cylindrical induction motor, it is proposed to approximate a 3D disk motor model by a 2D model of a standard cylindrical motor (2dRFIM – 2d Radial Flux Induction Machine). In the case of disk machines such approximation is not equivocal due to variable magnetic conditions along disk radii.

The correct representation of the electromagnetic circuit in a 2D model plane is the linear development of the cross-section at a selected equivalent radius (Fig. 2(b)). However, from a practical, i.e. designer's standpoint a much more feasible and effective procedure on account of simulation possibilities is to transfer a developed linear cross-section of the disk motor electromagnetic circuit onto the plane of a standard cylindrical motor (Fig. 2(c)). This method has been used e.g. in the work conducted by M. Valtonen and others [6, 12]; however, details of converting the linear circuit to the 2D plane of the cylindrical motor have not been presented and no verification of calculation results has been given. The cited authors have provided the sole information that the analysis had been run by the FEM using a 2D model of a motor; no additional details have been given. The current paper presents a very detailed procedure/algorithm for model preparation. The key principles of converting a 3D model into a cylindrical motor plane have been determined. Moreover, the proposed method of model elaboration has been verified using lab test results (on a physical motor model). The values of relative errors have been calculated and presented in the tabular form, for equivalent circuit parameters, rated parameters and operational parameters. Therefore, it has been possible to draw very specific conclusions on the limitations of the presented method, on account of the high divergence of results in some operational states of the motor.

The concept of an alternate computational method is discussed in the paper together with the elaborated rules for conversion of a disk motor's 3D model to a 2D model. The comparison of the obtained calculation results with the test results of the physical model has also been given.

2. The general idea of the presented method

The principle of operation as well as the equivalent scheme of a disk induction motor (Fig. 1) are the same as those of a standard induction cylindrical motor. The equivalent scheme is presented for a single phase. The main flux Φ and magnetizing current I_μ are represented in the scheme by magnetizing reactance X_μ . Resistance R_{Fe} represents stator core iron power losses X_μ and R_{Fe} parameters are voltage-dependent, so that they are connected in parallel to air-gap voltage

U_f in the scheme. To connect a rotor circuit with a stator circuit in a single equivalent scheme, rotor winding parameters must be expressed in terms of stator frequency f_1 . Such parameters are marked with apostrophes.

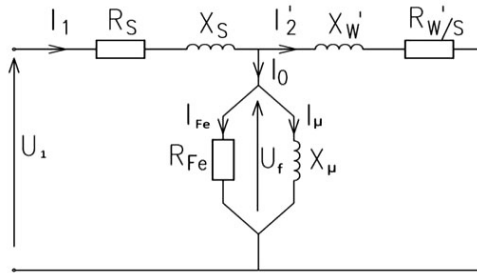


Fig. 1. Equivalent scheme of disk induction motor AFIM-11

$$U_1 = U_f + I_1 \cdot R_s + jI_1 \cdot X_s, \tag{1}$$

$$U_f = jI_2' \cdot X_w' + I_2' \cdot \frac{R_w'}{s}, \tag{2}$$

$$I_1 = I_2' + I_0, \tag{3}$$

where U_1 is the stator phase voltage, I_1 is the stator phase current, R_s is the stator phase resistance, X_s is the stator leakage reactance, R_{Fe} is the resistance representing stator iron core losses, X_μ is the magnetizing reactance, U_f is the air-gap voltage, I_0 is the idle run current, I_μ is the magnetizing current, I_{Fe} is the active component of idle run current, I_2' is the rotor current, X_w' is the rotor leakage reactance expressed in stator terms, R_w' is the rotor resistance expressed in stator terms, s is the slip.

Taking the above statements into consideration, it has been proposed to approximate a 3D model of a disk motor with a 2D model at a standard cylindrical motor plane. Specific rules should be used in the approximation, making it possible to represent near-real magnetic conditions. In the case of disk machines such approximation is not unequivocal, due to e.g. varying stator and rotor disk radii.

The general concept of converting a computational model in accordance with the proposed alternate method is visualized in Fig. 2. This presents the sequence of transfer from a 3D model to the linear model of the cross-section, and then “rolling” of the linear model into the geometry of a standard cylindrical motor. The block diagram of an alternate computational method algorithm is shown in Fig. 4. It must be noted that the conversion of the disk motor into the 2D cylindrical motor model is based upon the linear development of the cross-section. That is why we assume that all geometrical dimensions (used in the algorithm) for the model shown in Fig. 2(b) are known.

The key issue in the preparation of a 2dRFIM model is the elaboration of appropriate lamination shapes for a rotor and stator. The first step is the determination of so-called equivalent diameter D_{sr} . This diameter has often been adopted as half the sum of outer diameter D_z and inner diameter D_w [3, 7, 8]. In the discussed method a different division is proposed: the determined equivalent diameter of stator/rotor disks is the geometric diameter which halves the surface of the pole pitch.

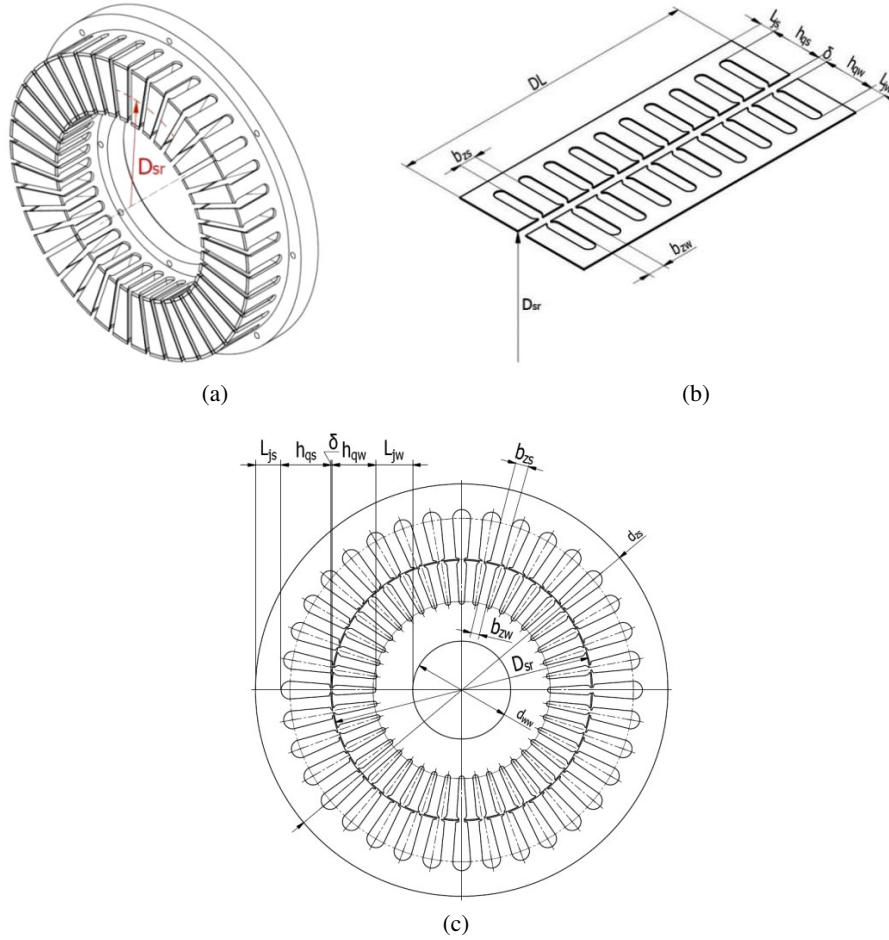


Fig. 2. Stages of converting electromagnetic circuit of disk model to 2D plane of cylindrical motor: (a) core of disk motor; (b) linear development of the stator/rotor cross-section at D_{sr} diameter; (c) 2D model at a plane of cylindrical motor

$$D_{sr} = \sqrt{\frac{D_z^2 + D_w^2}{2}}. \quad (4)$$

It is assumed that the equivalent diameter worked out in this way will lead to improved averaging of magnetic conditions. It must be noted here that the determined equivalent diameter D_{sr} is an outer diameter of a rotor in a 2dRFIM model; only then the circumference of the rotor lamination (Fig. 2(c)) and the length of linear development of cross-section DL (Fig. 2(b)) are equal as required.

When the outer rotor diameter is chosen, the appropriate design of stator slots and teeth is attempted. In the real disk motor, the stator/rotor tooth width differs depending on a given diameter. The slot width is constant and does not depend on the diameter. However, if the 2D

plane of linear development of the cross-section for the D_{sr} diameter is taken as reference and if we take into account the fact that rotating machines are usually designed so that the lamination teeth are convergent, the specified general dimension of rotor tooth width b_{zw} and stator tooth width b_{zs} may be adopted with values equal to those present in a linear development model of the cross-section (Fig. 2(b)). At this conversion stage, it is necessary to simplify matters, since it is not possible to keep the rotor tooth and slot width constant in a 2dRFIM model simultaneously. In order to obtain the magnetic flux and flux density distribution in different elements of a magnetic circuit as near to real values as possible, it is necessary to keep the tooth width constant; the width of the rotor slot will result from calculations. This sort of approach will cause the rotor slot dimensions to differ from real dimensions. Moreover, during the selection of rotor slot dimensions, we must take into account the rotor tooth height h_{qw} ; this height must be maintained equal to the real height of the tooth in the disk machine.

The last stage in the preparation of the rotor's magnetic circuit model is the selection of inner diameter. It would be appropriate to choose the diameter in such a way, that the real length of the magnetic path and yoke saturation level should be preserved. However, this is not possible since the values of the inner diameter in the 2dRFIM model are much less in relation to the D_{sr} diameter. That is why it is assumed that the rotor's inner diameter (and simultaneously yoke height) ought to be selected so that the magnetic voltage drop in the rotor yoke of the 2dRFIM model should be as close as possible to the voltage drop in the rotor yoke of the model shown in Fig. 2(b) (calculation of voltage drop takes into account the magnetizing curve of the sheets). So, if the calculated length of the magnetic path in the rotor yoke of the 2dRFIM model is decreased by half, then the average value of field intensity in the yoke should be increased twice. The average length of the magnetic path in the rotor yoke of the 2dRFIM model may be approximated from relationship:

$$l_{jw2dRFIM} = \frac{\pi \cdot (d_{ww} + L_{jw})}{2 \cdot p_b} + L_{jw}, \quad (5)$$

where

d_{ww} is the inner diameter of the rotor in the 2dRFIM model,

L_{jw} is the height of the rotor yoke in the 2dRFIM model and linear model of the cross-section,

p_b is the number of pairs of the magnetic poles.

The subsequent stage of conversion is the design of the stator core lamination shape for the 2dRFIM model, starting with selected outer rotor diameter d_{zw} . In this case, successive key dimensions, i.e. inner and outer stator diameters, result from summing different partial dimensions.

The following factors must be taken into consideration:

- real dimension of air-gap δ must be maintained,
- constant width of stator tooth (same as in case of rotor tooth) equal to b_{zs} must be maintained,
- real height of stator tooth (same as in case of rotor) equal to h_{qs} must be maintained,
- selection of a stator yoke must be carried out taking into account magnetic voltage drops (same as in the case of the rotor).

When geometric dimensions are defined, then stator and rotor winding parameters must be determined. Resistance of rotor end-rings must be assumed to be equal to the arithmetic mean of resistances for outer ring D_{pn1} and inner ring D_{pn2} . Apart from that, the remaining stator/rotor quantities should be defined in accordance with real values. At the last stage of the computational model preparation, analysis parameters and finite element mesh are defined. Examples of a computational model 2dRFIM and 3D model are shown in Fig. 3.

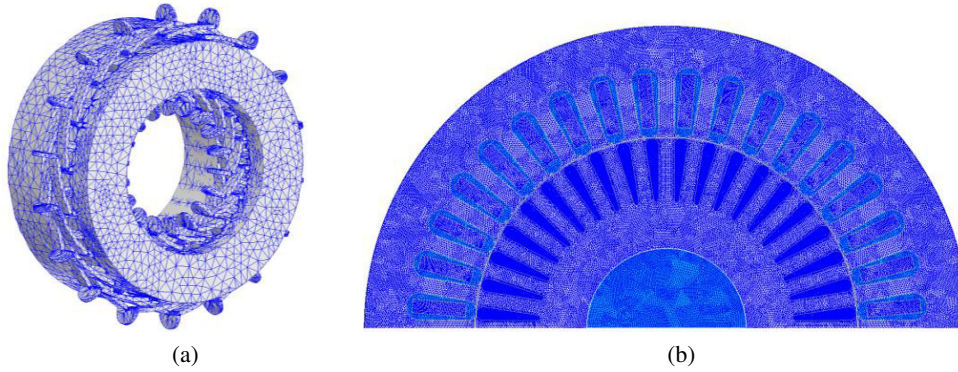


Fig. 3. (a) 3D model with a defined finite element mesh and (b) 2dRFIM computational model

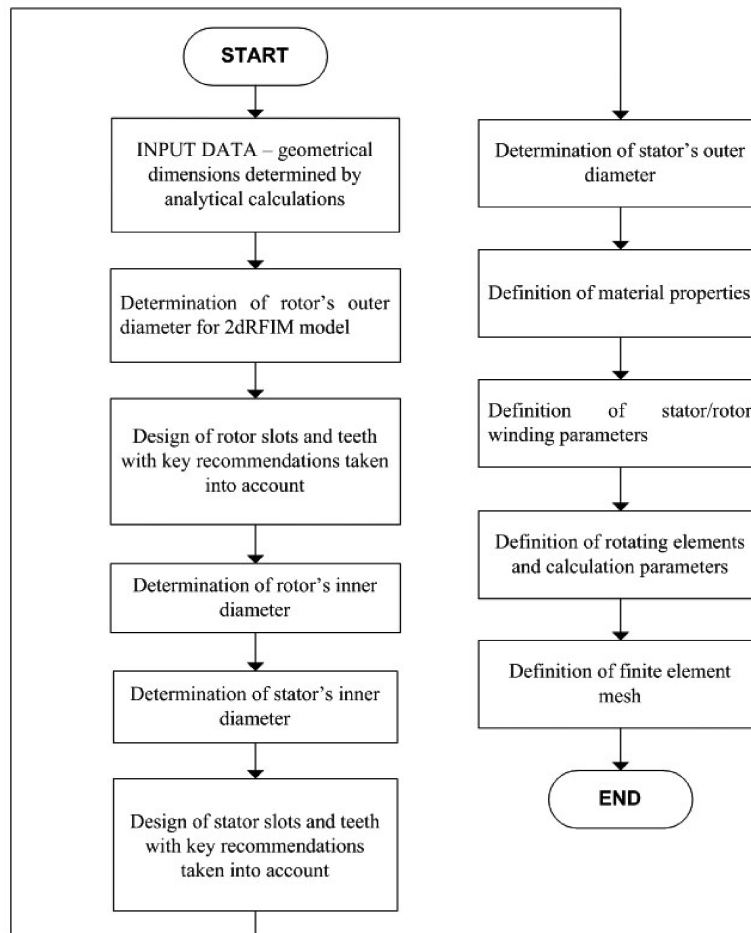


Fig. 4. Block diagram of the algorithm for 2D model of AFIM-11 motor development at a cylindrical motor plane

3. Key issues of converting 3D model of disk motor into 2D plane of cylindrical motor

The following key principles of converting a model of a disk induction motor electromagnetic circuit to a 2D model in the standard cylindrical motor plane have been established:

1. Rotor's outer diameter d_{zw} of a 2dRFIM model is equal to equivalent diameter D_{sr} .
2. Active length L of the 2dRFIM model is equal to $(D_{zs} - D_{zw})/2$.
3. Correction of rotor slot dimension is required, so that the width of rotor tooth b_{zw} is constant and equal to the real rotor tooth width at equivalent diameter D_{sr} .
4. Height of a stator/rotor slot is equal to real slot height h_{qs} and h_{qw} of a disk motor.
5. Height of a stator/rotor yoke is equal to real yoke height L_{js} and L_{jw} of the disk motor for machines with an unsaturated core.
6. When a stator or rotor core is saturated, it is necessary to calculate lengths of main flux magnetic paths in the rotor/stator yokes of the 2dRFIM with initially set dimensions d_{zs} and d_{ww} ; these dimensions should be then corrected in such a way, that the magnetic voltage drop in the rotor/stator yokes of the 2dRFIM model might be as close as possible to values present in the model of linear development of the cross-section.
7. Correction of stator slot dimensions is required so that stator tooth width b_{zs} might be constant and equal to the real stator tooth width at substitute diameter D_{sr} .
8. Resistance of end-rings of the 2dRFIM model is equal to the arithmetic mean of upper ring D_{pn1} and inner ring D_{pn2} .
9. On account of the decreased cross-section of the rotor slot in the 2dRFIM model, the value of rotor bar conductance γ_{pr} should be proportionately modified so that the active resistance of the rotor bar might not be changed in relation to the real model.
10. Air-gap length is equal to real air-gap length δ .

In relation to the real model of the disk motor electromagnetic circuit based on linear development of the cross-section, the 2dRFIM model exhibits the following differences:

1. In the cross-section linear development model, both slots and teeth are parallel and their values are constant. In the 2dRFIM model only stator/rotor teeth are parallel. This difference is shown graphically in Fig. 5.
2. Length of the magnetic path of the main flux in the rotor yoke of the 2dRFIM model is less than the corresponding length in the linear development of the cross-section model.
3. Length of the magnetic path of the main flux in the stator yoke of the 2dRFIM model is greater than the corresponding length in the linear development of the cross-section model.
4. The cross-section of the rotor slot in the 2dRFIM model is less than the cross-section of this slot in the linear development of the cross-section model.
5. The cross-section of the stator slot in the 2dRFIM model is greater than the cross-section of this slot in the linear development of the cross-section model.

The comparison (to scale) of stator/rotor slot dimensions in the computational model 2dRFIM in relation to real dimensions of slots in the physical model of the motor is shown in Fig. 5. Due to necessary correction of the dimensions, the cross-section of the stator slot in the 2dRFIM model is greater, and that of the rotor slot is less than in the real model.

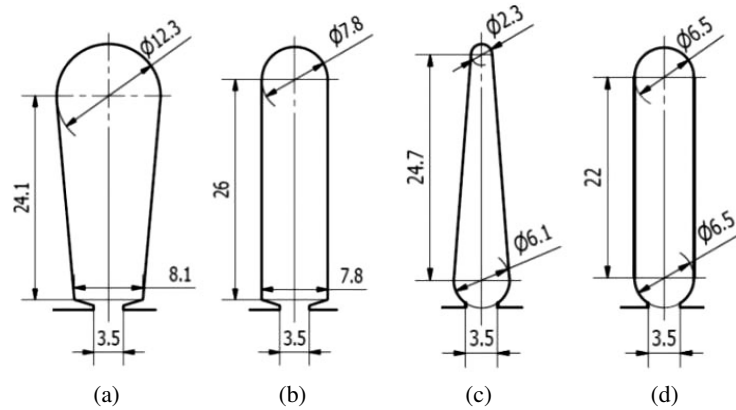


Fig. 5. Comparison (to scale) of stator slot dimensions (a, b) and rotor slot dimensions (c, d); computational model 2dRFIM (a, c) and real motor model (b, d)

4. Verification of alternate computational method

The calculation results obtained for the alternate computational method have been verified by lab test results acquired for the real model of the disk motor (Fig. 6). The comparison has been made for rated parameters as well as for equivalent scheme parameters of the motor at the rated supply conditions (400 V, 50 Hz). The basic data on dimensions of the magnetic circuit, winding and rated parameters of the tested motor is given in Table 1.

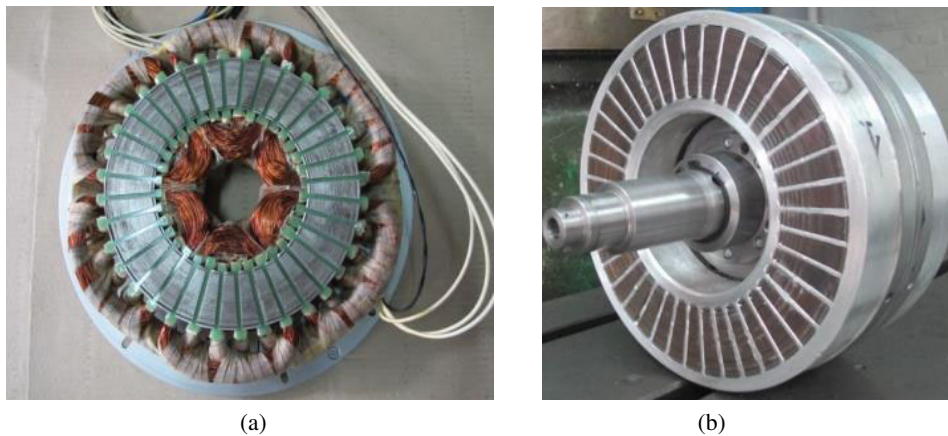


Fig. 6. Model of the motor: (a) stator with winding (b) rotor fitted with bearing into the shaft

Comparison of equivalent scheme parameters of disk motor AFIM-11 is presented in Table 2. The parameters have been obtained from calculations conducted with the discussed alternate method and directly or indirectly from lab tests run under rated supply parameters of the motor.

Table 1. Basic design data of model motor AFIM-11

Parameter			
Outer diameter – stator and rotor	D_z	[mm]	205
Inner diameter – stator and rotor	D_w	[mm]	130
Length of motor's magnetic circuit	L	[mm]	100
Air-gap length	δ	[mm]	0.85
Number of poles	$2p$	–	6
Number of stator phases	m	–	3
Number of stator slots	Q_s	–	36
Number of rotor slots	Q_w	–	40
Stator's winding factor	k_w	–	0.933
Rated voltage	U_{LL}	[V]	400
Rated frequency	f_s	[Hz]	50
Rated power	P_n	[W]	1500
Rated torque	T_n	[Nm]	15
Rated current	I_n	[A]	3.4

The values of relative errors for the alternate computational method have been calculated with the help of Formula (6).

$$\delta [\%] = \frac{|x - x_0|}{x} \cdot 100, \quad (6)$$

where x_0 is the calculated value, x is the value obtained directly or indirectly from lab tests.

Table 2. Parameters of equivalent scheme obtained for the alternate computational method and from lab test of real motor model

		2dRFIM model calculations	Tests	Relative error value
R_s	[Ω]	4.58	4.3	6.5%
$X_s + X'_w$	[Ω]	13.4	17.65	24.1%
R_{Fe}	[Ω]	2134	2078	2.7%
X_μ	[Ω]	124.2	113.8	9.1%
R'_w	[Ω]	2.82	3.24	13.0%

When the results for equivalent scheme parameters shown in Table 2 are analysed, we may observe that they show good convergence with the test results for the real model. The calculated relative error for most compared parameters varies from 6% to 13%. The highest difference (relative error *c.*25%) occurs in the case of the sum of stator/rotor leakage reactances. This is mostly due to necessary corrections of rotor and stator slot dimensions in a 2dRFIM model relative to real values. Differences between the calculated and measured reactance values will directly influence disparities in the obtained values of motor's maximum torque and slip corresponding to maximum torque.

Apart from the equivalent scheme parameters, a comparison has been run for motor's rated parameters at rated supply conditions (400 V, 50 Hz). The results are set out in Table 3. Additionally, the motor's characteristic parameters under specific operational conditions have also been considered (i.e. idle run current I_0 , start-up torque T_r , start-up current I_r , maximum torque T_k and slip corresponding to maximum torque s_k , input power P_1).

Table 3. Rated and operational parameters obtained from alternate computational method and from tests of real motor model

Rated parameters		2dRFIM model calculations	Tests	Relative error value
T_n	[N·m]	15	15.1	0.7%
P_1	[W]	1832	1882	2.7%
P_n	[W]	1514	1520	0.4%
I_n	[A]	3.21	3.71	13.5%
n	[rpm]	964	958	0.6%
$\cos \varphi$	–	0.805	0.73	10.3%
η	–	82.7%	80.8%	2.4%
Operational parameters				
I_0	[A]	1.77	1.87	5.3%
T_k	[N·m]	33.1	25.3	30.8%
s_k	–	0.17	0.13	30.8%
T_r	[N·m]	18.4	13.2	39.4%
I_r	[A]	15.1	11.5	31.3%

When the results shown in Table 3 are analysed, we may observe that in the range of rated parameters they show good convergence with the test results for the real model. The calculated relative error for most compared parameters is less than 5%; in the case of rated current I_n and power factor $\cos \varphi$ this error varies from 10 to 15%. However, a high discrepancy between the calculation results and lab test results is evident where operational parameters are concerned;

this is in particular true in the case of such parameters as maximum torque, slip corresponding to maximum torque and start-up current. The error is as high as 30–40%, which is unacceptable. Only in the case of idle run current, relative error is *c.* 5% and this is reasonable. It has been pointed out previously that these divergencies might be traced back to the introduced corrections of slot dimensions; these are directly responsible for leakage reactances' values.

5. Conclusions

Summarizing the issue of an alternate computational method for an induction disk motor in the 2D plane of a cylindrical motor, it must be acknowledged that the proposed method may be successfully used in the initial assessment of electromagnetic parameters of such machines. It must be noted that the obtained calculation results are characterized by satisfactory convergence in the linear range of the torque-speed curve, rated parameters included. The remaining operational parameters, maximum and start-up values mostly are burdened with relatively high error; therefore, they must be treated as a rough estimate only. Still, this method may be considered as a supplementary method, allowing a relatively fast determination of basic parameters of the electromagnetic circuit of a disk induction motor with a single stator and single rotor (AFIM-11).

Acknowledgements

The project has been financed by the Narodowe Centrum Nauki (National Science Centre) within the framework of the research grant no. UMO 2012/07/B/ST8/04099.

References

- [1] Śliwiński T., *Design methods of induction motors, part I. Analysis*, Wydawnictwo Naukowe PWN, (in Polish – Metody obliczania silników indukcyjnych t.1 Analiza) (2008).
- [2] Głowacki A., *Electromagnetic calculations of three-phase induction motors*, Wydawnictwo Naukowo-Techniczne, in Polish (Obliczenia elektromagnetyczne silników indukcyjnych trójfazowych) (1993).
- [3] Parviainen A., *Design of axial-flux permanent-magnet low-speed machines and performance comparison between radial-flux and axial flux machines*, PhD Thesis, Lappeenranta teknillinen yliopisto, Digipaino (2005).
- [4] Mendrela E., Łukaniszyn M., Macek-Kamińska K., *Disk direct current motors with electronic commutation*, Gnome – Wydawnictwa Naukowe i Artystyczne, in Polish (Tarczowe silniki prądu stałego z komutacją elektroniczną) (2002).
- [5] Łukaniszyn M., Wróbel R., Jagieła M., *Computer modeling of brushless disk motors excited with permanent magnets*, Oficyna Wydawnicza Politechniki Opolskiej, in Polish (Komputerowe modelowanie bezszczotkowych silników tarczowych wzbudzanych magnesami trwałymi) (2002).
- [6] Valtonen M., *Performance characteristics of an axial-flux solid-rotor-core induction motor*, PhD Thesis, Lappeenranta teknillinen yliopisto, Digipaino (2007).
- [7] Gieras J., Wang R., Kamper M., *Axial Flux Permanent Magnet Brushless Machines*, Kluwer Academic Publishers (2004).
- [8] Gieras J., Wing M., *Permanent magnet motor technology – Design and Applications*, Marcel Dekker (2002).

-
- [9] Caricch F., Crescimbin F., Santini E., *Axial-flux electromagnetic differential induction motor*, in Proc. of IEEE International Conference on Electrical Machines and Drives, Durham (1995).
 - [10] Nasiri-Gheidari Z., Lesani H., *A survey on Axial Flux Induction Motor*, Przegląd Elektrotechniczny (Electrical Review), pp. 300–305 (2012).
 - [11] Valtonen M., Parviainen A., Pyrhonen J., *Influence of the Air-Gap Length to the Performance of an Axial-Flux Induction Motor*, in Proc. of IEEE International Conference on Electrical Machines (ICEM), Vilamoura, Portugal (2008).